

Correlated domain model of deuterated dipole glass

Bog-Gi Kim

*Department of Physics, Korea Advanced Institute of Science and Technology, 373-1 Kusung-dong,
Yusung-ku, Taejon 305-701, Korea
and Laboratory for Physics/Chemistry of Dielectric Materials, Pohang University of Science and Technology,
Pohang 790-784, Korea*

Jong-Jean Kim

*Department of Physics and Center for Molecular Science, Korea Advanced Institute of Science and Technology, 373-1 Kusung-dong,
Yusung-ku, Taejon 305-701, Korea*

Hyun M. Jang

*Laboratory for Physics/Chemistry of Dielectric Materials, Pohang University of Science and Technology,
Pohang 790-784, Korea*

(Received 19 March 1999)

The low-frequency dielectric relaxation of the deuterated rubidium ammonium dihydrogen phosphate (DRADP) dipole glass was investigated by examining the complex dielectric permittivity above the glass freezing temperature. We show that none of the well-known Debye-type relaxation functions that include the Cole-Cole, Cole-Davidson, and Kohlrausch-Williams-Watts functions adequately describe the observed dielectric relaxation behavior of the DRADP. We then examine the Chamberlin's correlated domain model as a possible description of the DRADP dipole glass. The experimental data and the computational results based on the correlated domain model qualitatively agree with each other with common features of (i) a long tail at the lower-frequency side and (ii) increase in the asymmetry of $\epsilon''(\omega)$ spectrum with decreasing temperature. Finally, we discuss the fitting results of the DRADP dipole glass in comparison with glass-forming liquids and other polar glasslike systems. [S0163-1829(99)03034-9]

I. INTRODUCTION

In 1982, Courtens¹ reported glassy behavior of dipoles in a mixed crystal of ferroelectric rubidium dihydrogen phosphate (RDP) and antiferroelectric ammonium dihydrogen phosphate (ADP). After his pioneering work, considerable research efforts have been made to understand the nature of dipole glass and the main difference between the dipole glass and the well-studied spin glass.²⁻⁸ Compared to the spin glass system, there exists a strong coupling between the electric dipole and the lattice ion in the dipole glass system.^{1,2,5} In view of this, the formation of the dipole glass phase can be understood in terms of the frustrated correlation between the dipoles and the strong coupling via random fields. Therefore, the dipole glass system is now regarded as a model system for the theoretical understanding of glass freezing phenomena.

Freezing dynamics of the dipole glass system approaching the freezing temperature can be studied by broad-band dielectric spectroscopy.^{2,9-12} Courtens² studied the anomalous dispersion of dielectric loss which was contributed by a broadening of relaxation-time distribution. Using the Vogel-Fulcher analysis that had been successfully applied to many glass-forming liquid systems, he showed that the characteristic relaxation time of the dipole glass could be infinite at a finite temperature.

For the study of the divergence of relaxation time near the freezing temperature, the low-frequency dielectric spectroscopy is becoming an important tool because a lower fre-

quency implies a higher relaxation-time domain.^{9,10} Kuntjak and co-workers^{11,12} measured the relative dielectric permittivity of a deuterated mixed crystal of RDP and ADP (DRADP) down to 1 mHz. Assuming a simple linear form for the relaxation-time distribution function, they demonstrated that the lowest part of the relaxation frequency went to zero according to the Vogel-Fulcher law. More recently, using the DSP lock-in amplifier technique Kim and Kim¹³ have precisely measured the relative dielectric permittivity of the DRADP dipole glass system. Using the Tikhonov regularization method, they successfully obtained the relaxation-time distribution function without assuming a plausible functional form beforehand.¹³

Another important progress in the description of the relaxation behavior was made by Chamberlin.¹⁴ His approach is called the dynamically correlated domain model and is based on the idea that the relaxation of a domainlike particle refers to the transition between excited states toward the ground state via emission of elementary excitations (phonons, magnons, etc.). He applied this idea to the descriptions of magnetic relaxation,¹⁴ glass-forming liquid,^{15,16} amorphous system,¹⁷ and quadrupolar system.¹⁸ In this article we will apply this approach to examine the relaxation behavior of the DRADP dipole glass and discuss a possible difference between the dipole glass and other glasslike random systems.

In Sec. II, we will examine various empirical modifications of the Debye relaxation function by the integral transformation into the time-domain. These include the Cole-

Cole, the Cole-Davidson, and the KWW (Kohlrausch-Williams-Watts) functions. We will show that none of these functions adequately describes the observed dielectric relaxation behavior of the DRADP. As a non-Debye type relaxation, we will then examine the Chamberlin's correlated domain model in Sec. III. Finally, we will present the fitting results of the DRADP dipole glass and discuss the validity and the limitations of the correlated domain model for the description of the relaxation behavior of the DRADP dipole glass.

II. DIPOLAR RELAXATION

When the polarization $P(t)$ undergoes a dielectric relaxation toward the equilibrium state, its time-dependence can be described by the following first-order differential equation¹⁹

$$\frac{1}{\mu_d} \frac{dP(t)}{dt} + P(t) = \lim_{t \rightarrow \infty} P(t), \quad (1)$$

where $1/\mu_d$ is the characteristic relaxation time. Relaxation behavior can be studied either by monitoring the polarization switching current in the time domain or by measuring the complex dielectric permittivity in the frequency domain.

If we apply a static field V_0 , the steady-state solution of Eq. (1) becomes

$$P(t) = P_0 \exp(-\mu_d t), \quad (2)$$

where the switching current $I(t)$ is given by

$$I(t) = \frac{dP(t)}{dt} = -\mu_d P_0 \exp(-\mu_d t). \quad (3)$$

Equation (3) indicates that, for a single Debye relaxation, the switching current follows a simple exponential decay.

Alternatively, the relaxation behavior can be described by a dielectric dispersion relation in the frequency domain. For the Debye relaxation, the frequency-dependent complex dielectric permittivity $\epsilon^*(\omega)$ is given by

$$\epsilon^*(\omega) - \epsilon_\infty = \frac{\epsilon_0 - \epsilon_\infty}{1 + i\omega\tau_d}, \quad (4)$$

where ϵ_0 and ϵ_∞ are the static dielectric permittivity and the dielectric permittivity at an infinite frequency, respectively, and $\tau_d (= 1/\mu_d)$ is the characteristic relaxation time.^{19,20} The relaxation strength ϵ_s is defined as $\epsilon_0 - \epsilon_\infty$ and is related to P_0 by

$$\epsilon_s = \epsilon_0 - \epsilon_\infty = \frac{P_0}{V_0 C_0}, \quad (5)$$

where C_0 is the geometric capacitance of the sample and V_0 is the amplitude of a static field employed in the time-domain measurement. The relative permittivity at an infinite frequency ϵ_∞ , whose time constant is much shorter than the characteristic relaxation time for dipolar relaxation, is independent of the dipolar relaxation mechanism but is related to the instantaneous polarization (P_i) through $\epsilon_\infty = P_i/V_0 C_0$.

The complex dielectric permittivity can be written as the Fourier transform of the relaxation function,^{21,22} namely,

$$\epsilon^*(\omega) - \epsilon_\infty = - \int \frac{I(t)}{V_0 C_0} \exp(i\omega t) dt. \quad (6)$$

The above equation implies that the dielectric permittivity at a given frequency depends on the relaxation current around a time corresponding to the reciprocal of the chosen frequency ω . In a real system, the dielectric dispersion is usually characterized by the distribution of relaxation times. The mean value of the distribution function is related to the inertia of dipole moments. There are two approaches to the description of dielectric relaxation in a real system: One is an empirical modification of $P(t)$ or $\epsilon^*(\omega)$ and the other is an integral representation.

One of the well-known empirical modifications in the time-domain is the so-called KWW (Kohlrausch-Williams-Watts) function,^{23,24} namely,

$$P(t) = P_0 \exp[-(\mu t)^\beta] \quad (7)$$

where β is a constant having values between 0 and 1, and $\beta=1$ corresponds to a single Debye relaxation. The two most representative empirical modifications of the Debye equation in the frequency-domain are the Cole-Davidson function and the Cole-Cole function,^{21,25} and they are respectively given by the following two relations:

$$\epsilon^*(\omega) - \epsilon_\infty = \frac{\epsilon_0 - \epsilon_\infty}{(1 + i\omega\tau_0)^\beta}, \quad (8)$$

$$\epsilon^*(\omega) - \epsilon_\infty = \frac{\epsilon_0 - \epsilon_\infty}{[1 + (i\omega\tau_0)^{1-\alpha}]}, \quad (9)$$

where $1-\alpha$ or β is a measure of the deviation from the Debye relaxation. Another useful function that has been frequently used to represent the dielectric relaxation behavior in the frequency-domain is the Havriliak-Negami function²⁶⁻²⁹ defined by

$$\epsilon^*(\omega) - \epsilon_\infty = \frac{\epsilon_0 - \epsilon_\infty}{[1 + (i\omega\tau_0)^\alpha]^\beta}, \quad (10)$$

where α and β respectively represent the width and the skewness of the dielectric loss when viewed in a $\ln(\omega)$ plot.

Contrary to the empirical modifications discussed above, one can alternatively express the frequency-dependent complex dielectric permittivity using a concept of the relaxation-time distribution in the Debye relaxor, namely,

$$\epsilon^*(\omega) - \epsilon_\infty = (\epsilon_0 - \epsilon_\infty) \int \frac{g(\tau)}{1 + i\omega\tau} d(\tau), \quad (11)$$

where $g(\tau)$ is the relaxation-time distribution function which satisfies the normalization condition, $\int g(\tau) d(\tau) = 1$. Equation (11) signifies that the complex dielectric permittivity is an integral transformation of $g(\tau)$ using a kernel, $1/(1 + i\omega\tau)$. In this case, the polarization switching current can be written as

$$I(t) = \frac{dP(t)}{dt} = - \int f(\mu) \mu P_0 \exp(-\mu t) d(\mu), \quad (12)$$

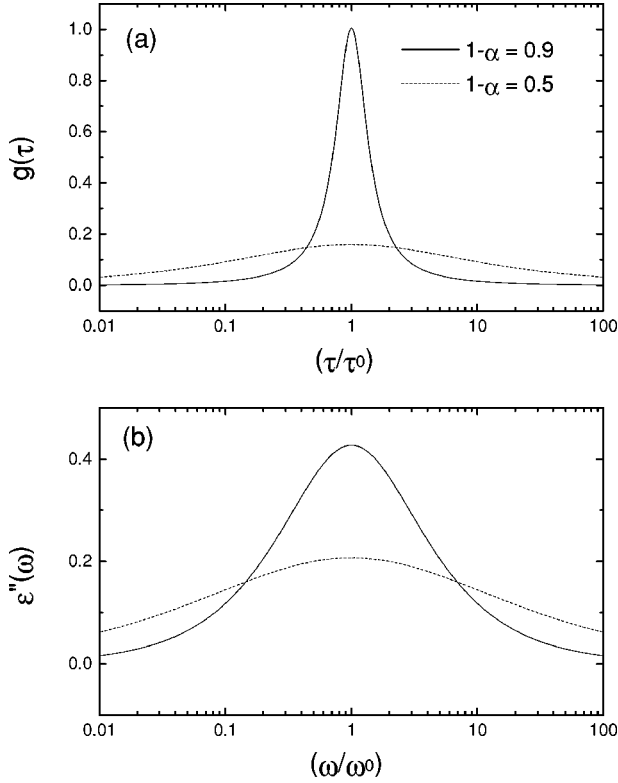


FIG. 1. Dielectric relaxation characteristics of the Cole-Cole function for two different values of α : (a) the relaxation-time distribution function $g(\tau)$, (b) the complex dielectric permittivity $\epsilon''(\omega)$.

where $f(\mu)$ represents the distribution of relaxation frequencies and satisfies the condition that $\int f(\mu)d(\mu) = 1$.

We are now in a position to find $g(\tau)$ for the two representative empirical modifications of the Debye equation (i.e., Cole-Cole and Cole-Davidson functions) by the integral transformation. To do this, let us first consider the complex dielectric permittivity in the Cole-Cole modification. The complex permittivity $\epsilon^*(\omega)$ can be separated into the real and imaginary parts, namely,

$$\frac{\epsilon'(\omega) - \epsilon_\infty}{\epsilon_0 - \epsilon_\infty} = \frac{1}{2} \left[1 - \frac{\sinh[(1-\alpha)x]}{\cosh[(1-\alpha)x] + \cos[\alpha\pi/2]} \right], \quad (13)$$

$$\frac{\epsilon''(\omega)}{\epsilon_0 - \epsilon_\infty} = \frac{1}{2} \frac{\cos[\alpha\pi/2]}{\cosh[(1-\alpha)x] + \cos[\alpha\pi/2]},$$

where $x = \ln(\omega\tau_0)$. On the analogy of the integral transformation given in Eq. (11) one can deduce the following relation for the relaxation-time distribution function using Eq. (13):

$$g(\tau) = \frac{1}{2\pi\tau} \frac{\sin(\alpha\pi)}{\cosh[(1-\alpha)\ln(\tau/\tau_0)] - \cos(\alpha\pi)}. \quad (14)$$

The distribution function $g(\tau)$ corresponding to the Cole-Cole relaxation is plotted in Fig. 1(a) as a function of (τ/τ_0) for two different values of α . Similarly, the imaginary part of the complex dielectric permittivity can be computed using Eq. (13) and presented in Fig. 1(b) as a function of (ω/ω_0) . The most prominent feature shown in Fig. 1 is that both $g(\tau)$

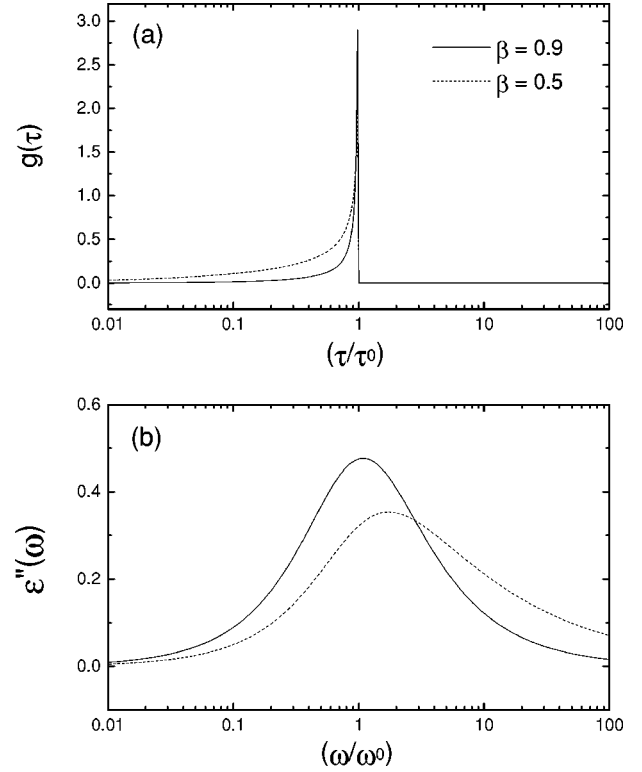


FIG. 2. Dielectric relaxation characteristics of the Cole-Davidson function for two different values of β : (a) the relaxation-time distribution function $g(\tau)$, (b) the complex dielectric permittivity $\epsilon''(\omega)$.

and $\epsilon''(\omega)$ are symmetric with respect to the reduced relaxation time τ_0 and ω_0 , respectively, when plotted in logarithmic scale. As can be noticed from Fig. 1, both functions become broader and deviate from the single Debye relaxor with increasing value of α . However, the average relaxation time is independent of α and is equal to τ_0 by virtue of the symmetry.

Similarly, $g(\tau)$ for the Cole-Davidson relaxation can be obtained by expanding the complex dielectric permittivity function, namely,

$$\frac{\epsilon^*(\omega) - \epsilon_\infty}{\epsilon_0 - \epsilon_\infty} = \frac{1}{(1 + i\omega\tau_0)^\beta} = \frac{1}{[\sqrt{1 + (\omega\tau_0)^2} \cdot e^{i\theta}]^\beta}, \quad (15)$$

where $\theta = \tan^{-1}(\omega\tau_0)$. One can eventually obtain the following distribution function for the Cole-Davidson relaxation

$$g(\tau) = \frac{\sin(\beta\pi)}{\pi} \left(\frac{\tau}{\tau_0 - \tau} \right)^\beta \quad \text{for } \tau < \tau_0, \quad (16)$$

$$g(\tau) = 0 \quad \text{for } \tau > \tau_0.$$

We present both $g(\tau)$ and $\epsilon''(\omega)$ for the Cole-Davidson function in Fig. 2. In this case, $g(\tau)$ has a long tail in the lower part of τ and discontinuously becomes 0 at $\tau = \tau_0$. On the other hand, $\epsilon''(\omega)$ stretches into the high-frequency region with decreasing β . Because of this type of the asymmetry, the average relaxation time should be written as $\langle \tau \rangle_{CD} = \tau_0 \times \beta$. Since the Havriliak-Negami function is a combina-

tion of the Cole-Cole and Cole-Davidson functions [Eq. (10)], one can readily show that $\epsilon''(\omega)$ also has a long tail in the high-frequency side.

Finally, let us consider the complex permittivity function corresponding to the KWW function. Since the KWW function describes the dielectric relaxation in the time-domain, one can establish the following relation for the complex dielectric permittivity:²¹

$$\begin{aligned} \frac{\epsilon^*(\omega) - \epsilon_\infty}{\epsilon_0 - \epsilon_\infty} &= \int \exp(-i\omega t) \left(-\frac{d}{dt} P(t) \right) dt \\ &= \int \frac{g(\tau)}{1 + i\omega\tau} d\tau, \end{aligned} \quad (17)$$

where $P(t) = \exp[-(t/\tau_{ww})^{\beta_{ww}}]$. Using Eq. (17) one can deduce the relationship between $P(t)$ and $g(\tau)$ as

$$P(t) = \exp[-(t/\tau_{ww})^{\beta_{ww}}] = \int \exp(-t/\tau) g(\tau) d\tau. \quad (18)$$

Thus, the time-dependent polarization is the Laplace transform of the distribution function $g(\tau)$. Using the inverse Laplace transform one can obtain an analytic solution of $g(\tau)$. For this purpose, let us first introduce the following set of variables:

$$x = \tau_{ww} / \tau, \quad (19)$$

$$s = t / \tau_{ww},$$

$$\beta = \beta_{ww},$$

$$\lambda(x, \beta) = \frac{\tau_{ww}}{x^2} g\left(\frac{\tau_{ww}}{x}\right).$$

Using these definitions one can rewrite Eq. (18) as

$$\exp(-s^\beta) = \int \exp(-sx) \lambda(x, \beta) dx. \quad (20)$$

The analytic solution of $\lambda(x, \beta)$, thus, $g(\tau)$ is given by

$$\lambda\left(x, \frac{1}{2}\right) = \frac{1}{2\sqrt{\pi}} x^{-3/2} \exp(-0.25x), \quad (21)$$

$$\begin{aligned} \lambda(x, \beta) &= \frac{1}{\pi} \int \exp(-xu) \exp[-u^\beta \cos(\pi\beta)] \\ &\quad \times \sin[u^\beta \sin(\pi\beta)] du, \end{aligned}$$

$$\lambda(x, \beta) = -\frac{1}{\pi} \sum_k (-1)^k \sin(\pi\beta k) \frac{\Gamma(\beta k + 1)}{\Gamma(k+1) x^{\beta k + 1}},$$

where Γ denotes the gamma function. The complex dielectric permittivity can be obtained using a series expansion of the gamma function, namely,

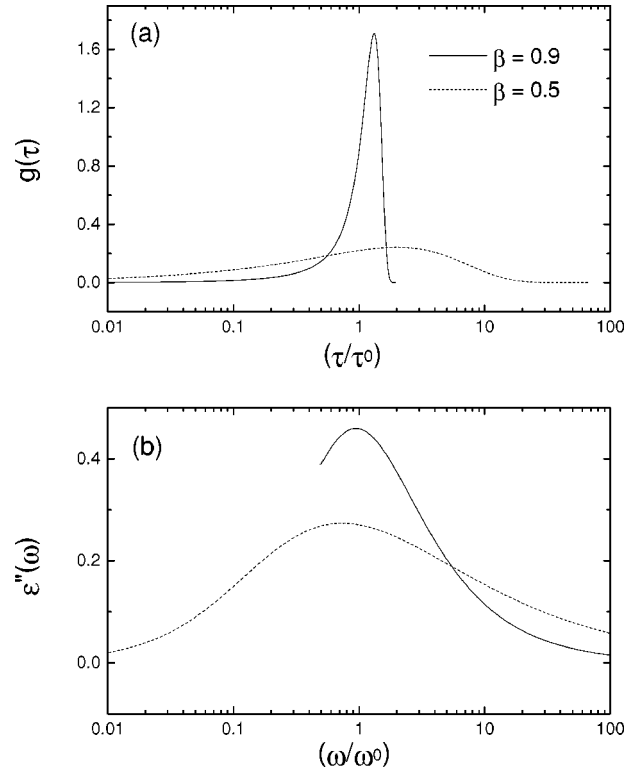


FIG. 3. Dielectric relaxation characteristics of the KWW function for two different values of β : (a) the relaxation-time distribution function $g(\tau)$, (b) the complex dielectric permittivity $\epsilon''(\omega)$.

$$\begin{aligned} \frac{\epsilon^*(\omega) - \epsilon_\infty}{\epsilon_0 - \epsilon_\infty} &= \sum_k (-1)^{k-1} \frac{\Gamma(\beta_{ww} k + 1)}{\Gamma(k+1)} \\ &\quad \times \frac{1}{(\omega \tau_{ww})^{\beta_{ww} k}} \exp\left(-i \frac{\pi \beta_{ww} k}{2}\right). \end{aligned} \quad (22)$$

The convergence of $g(\tau)$ and $\epsilon''(\omega)$ is good for $\tau < \tau_{ww}$ but becomes very poor for $\tau > \tau_{ww}$.

$g(\tau)$ and $\epsilon''(\omega)$ for the KWW function are presented in Fig. 3. The distribution function $g(\tau)$ has a long tail in the lower part of τ but $\epsilon''(\omega)$ stretches into the high-frequency region with decreasing β . Therefore, the dielectric relaxation characteristics of the KWW function are similar to those of the Cole-Davidson function. Because of the asymmetry, the average relaxation time and its higher moments are not equal to τ_{ww} and $(\tau_{ww})^n$, respectively, but should be written as

$$\langle \tau \rangle_{ww} = \frac{\tau_{ww}}{\beta_{ww}} \Gamma\left(\frac{1}{\beta_{ww}}\right) \quad \text{and} \quad \langle \tau^n \rangle_{ww} = \frac{(\tau_{ww})^n}{\beta_{ww}} \frac{\Gamma(n/\beta_{ww})}{\Gamma(n)}. \quad (23)$$

We have systematically investigated dielectric properties of the deuterated rubidium ammonium dihydrogen phosphate mixed crystal $[\text{Rb}_{1-x}(\text{ND}_4)_x\text{D}_2\text{PO}_4]$ (DRADP- x) with $x = 0.4$ for a wide range of frequency. It was shown that the dielectric response of the DRADP-0.4 dipole glass did not follow the single Debye relaxation as temperature went down to the glassy freezing temperature.¹³ In this study we have further found that the imaginary part of the complex dielectric permittivity of the DRADP-0.4 has a long tail in the low-frequency region. As discussed in this section, for

the Cole-Cole-type relaxation both $g(\tau)$ and $\epsilon''(\omega)$ are symmetric with respect to the reduced relaxation time τ_0 and ω_0 , respectively, when plotted in logarithmic scale. We have also shown that all three remaining relaxation functions, i.e., Cole-Davidson, Havriliak-Negami, and KWW, have a common feature of a long tail in the high-frequency side of $\epsilon''(\omega)$. Therefore, none of these four relaxation functions can adequately describe the dielectric relaxation behavior of the DRADP dipole glass. In view of this, as briefly mentioned in the Introduction, we have investigated the correlated domain model as a possible description of the DRADP dipole glass.

III. CHAMBERLIN'S CORRELATED DOMAIN MODEL

Dynamically correlated domain is defined as a region where the dispersive excitations have a common dynamic phase factor and, thus, relaxes uniformly with a single relaxation rate. Therefore, all the dipoles (or spins) within the correlated domain have the same average level of excitation.¹⁴⁻¹⁸ Since the initial response (P_s) and the relaxation rate (ω_s) are directly related to the size of a given correlated domain, the net response $P(t)$ can be written using the following linear response terms with the weighted sum over all the domains:

$$P(t) = \sum_s n_s P_s \exp(-t\omega_s), \quad (24)$$

where n_s is the size distribution function.

Now, let us consider the two size-dependent functions in Eq. (24). It seems reasonable that P_s is proportional to the size (s) of the domain because the initial response per dipole (or spin) can be assumed to be homogeneous throughout a given correlated domain. On the other hand, ω_s can be written as $\omega_s \propto \exp(-\delta E_s/k_B T)$ if one assumes that the relaxation rate of each domain does obey the thermally activated Arrhenius behavior. The excitation density of states can be assumed to be proportional to the volume of a given domain so that the energy level spacing is given by $\delta E_s = \pm \Delta/s$, where Δ is related to the energy bandwidth. The relaxation rate then becomes $\omega_s \propto \exp(-\alpha/s)$, where the dimensionless energy ratio α is defined as $\alpha = \delta E_s s/k_B T$.

Using the above arguments and replacing a discrete variable s to a continuous variable x , one can rewrite the weighted response function $P(t)$ as the following integral form:

$$P(t) \propto \int_D x n_x \exp(-t\omega_x) dx, \quad (25)$$

where $\omega_x = \omega_0 \exp(-C/x)$, ω_0 is an asymptotic relaxation rate, and C is a coefficient representing the degree of the dynamic dipolar correlation. The complex dielectric permittivity is the Fourier transform of time derivative of the response function given in Eq. (25), namely,

$$\epsilon^*(\omega) \propto \int_D x n_x \frac{dx}{1 + i\omega/\omega_x}. \quad (26)$$

Comparing Eq. (26) with Eq. (11), one can deduce that $x n_x$ is nothing but the distribution function of the relaxation time, and ω_x has the same meaning as $1/\tau$.

We now consider n_x . Chamberlin proposed two distinct size distribution functions for the dynamically correlated domains. One is a normal Gaussian distribution function, which is valid for an ergodic system governed by the central limit theorem:

$$n_x \propto \exp[-(x-x_0)^2]. \quad (27)$$

The other is a Poisson distribution obtained using the bond-percolation theory. Therefore, this type of distribution function is relevant to a glass-like system having a quenched randomness:

$$n_x \propto x^{1/9} \exp[-x^{2/3}]. \quad (28)$$

Since dipole glass has a quenched randomness, one can obtain the following expression for the complex dielectric permittivity after combining Eq. (28) with Eq. (26):

$$\epsilon^*(\omega) = A \int_D x^{10/9} \exp(-x^{2/3}) \frac{dx}{1 + i\omega/\omega_x}, \quad (29)$$

where A is a parameter that represents the dipolar strength $\Delta \epsilon$. The line shape of the permittivity spectrum is, therefore, determined by ω_x which is defined as $\omega_x = \omega_0 \exp(-C/x)$, as discussed in Eq. (25).

IV. RESULTS AND DISCUSSION

In Sec. II, we examined all of the four important empirical modifications of the Debye relaxation (Cole-Cole, Cole-Davidson, Havriliak-Negami, and KWW functions) and found that none of these functions adequately describes the experimental dielectric relaxation behavior of the DRADP dipole glass. Then, we subsequently examined the Chamberlin's correlated domain model as a possible model of the dipole glass in the previous section. In this section, we will test the validity of the correlated domain model for the description of dielectric behavior of the DRADP dipole glass and discuss the main difference between the dipole glass and other random systems, especially a glass-forming liquid.

To do this, let us reconsider Eq. (29) first. As discussed in Eq. (25), the coefficient C represents the degree of the dynamic correlation between dipoles. In case of $C=0$, ω_x becomes ω_0 irrespective of the value of x since $\omega_x = \omega_0 \exp(-C/x)$. Then, substituting $1/\tau$ for ω_0 , one can realize that the imaginary part of the dielectric permittivity is given by the integral representation of simple Debye-type relaxors, namely,

$$\epsilon''(\omega) = A \int_D dx x^{10/9} \exp(-x^{2/3}) \frac{\omega \tau}{1 + (\omega \tau)^2}. \quad (30)$$

In this case, all the constituting domains are the independent Debye relaxors with the same relaxation frequency, and the distribution function of the Debye relaxors is the same as the domain-size distribution, i.e., Poisson-like distribution.

When C is not equal to zero, the sign of C actually determines the line shape of the dielectric permittivity spectrum. In case of $C < 0$, the imaginary part of the dielectric permittivity has a long tail in the high-frequency side. On the other hand, it has a long tail in the low-frequency region for $C > 0$. As discussed in Sec. II, the complex dielectric permit-

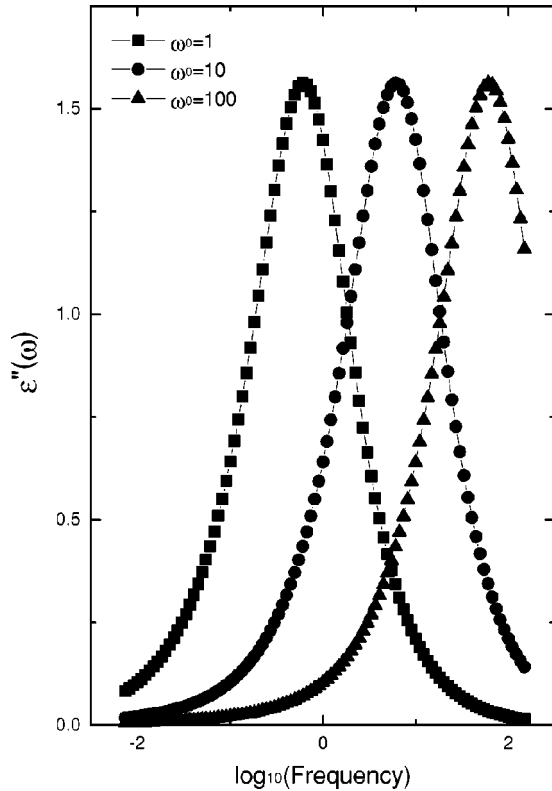


FIG. 4. The variation of the simulated $\epsilon''(\omega)$ plotted as a function of frequency for three different values of ω_0 .

tivity of the DRADP dipole glass has a long tail in the low-frequency region. Therefore, the condition of $C > 0$ is appropriate for the relaxation of dipoles in the DRADP.

We now examine the effects of the two important parameters, ω_0 and C (with positive values), on the shape of the complex dielectric permittivity function. Let us first consider the asymptotic relaxation rate, ω_0 . Figure 4 shows the variation of the simulated $\epsilon''(\omega)$ as a function of frequency for three different values of ω_0 . The parameters A and C used in the computation are 1 and 2, respectively. One can make the following three important conclusions from the inspection of the result shown in Fig. 4: (i) The frequency-dependent dielectric response is nearly the same as that of the single Debye relaxor for a small positive value of C . (ii) The width of the permittivity function is independent of ω_0 for a given value of C . (iii) The value of ω_0 actually determines the frequency at which $\epsilon''(\omega)$ shows its maximum, ω_{max} .

Figure 5 shows the effect of the coefficient of dynamic correlation, C , on the simulated $\epsilon''(\omega)$ for $A = 1$ and $\omega_0 = 1$. The extent of the shift toward the low-frequency region with the appearance of a tail in the low-frequency side increases as C increases or as the coupling between the dipoles becomes stronger. One can obtain the following conclusion by comparing the result of Fig. 5 with that of Fig. 4: Because the width of $\epsilon''(\omega)$ spectrum is independent of ω_0 , both the asymmetry and the width of $\epsilon''(\omega)$ are solely determined by the degree of the dynamic correlation between dipoles, C .

Let us now examine the validity and the limitations of the correlated domain model for the description of the relaxation behavior of the DRADP by a numerical fitting of the experimental results. The algorithm used in the present study is the method of the multidimensional minimization using the

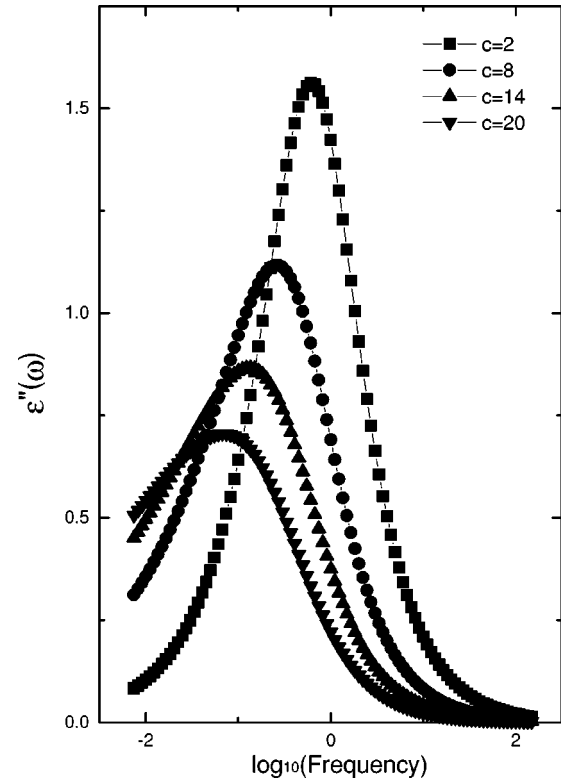


FIG. 5. The variation of the simulated $\epsilon''(\omega)$ plotted as a function of frequency, showing the effect of the dynamic dipolar correlation (C) on the simulated $\epsilon''(\omega)$ spectrum.

Powell method of the *Numerical Recipes in C*.³⁰ For the integration, the qromo method of the *Numerical Recipes in C* (Ref. 30) was used. It took approximately three hours for each numerical fitting of the complex permittivity function. Various initial conditions were tested to prevent the function from tapping in a local minimum. When we obtained the same final result irrespective of the initial condition employed, we judged that the function reached its global minimum.

Figure 6 compares the numerically obtained functions (continuous solid lines) with the experimental dielectric permittivity at four different temperatures. Although there are some discrepancies between the computational results and the experimental data,¹³ both of them have the same general tendencies: (i) a long tail at the lower-frequency side and (ii) increase in the asymmetry of $\epsilon''(\omega)$ spectrum with decreasing temperature. Because we were trying to get the best fitting at the low-frequency region, the discrepancies between these two results became pronounced at the high-frequency side.

The three physically important parameters used in the present correlated domain model have been obtained for various temperatures by the numerical fitting, and they are presented in Fig. 7. As shown in Fig. 7(a), the amplitude parameter A is essentially constant with its mean value around 20 or tends to decrease slightly with decreasing temperature. This suggests that the dipolar strength $\Delta\epsilon$ is little affected by temperature. Figure 7(b) shows that $\ln(\omega_0)$ increases almost linearly with the absolute temperature. This predicts that the Debye frequency of the dynamically corre-

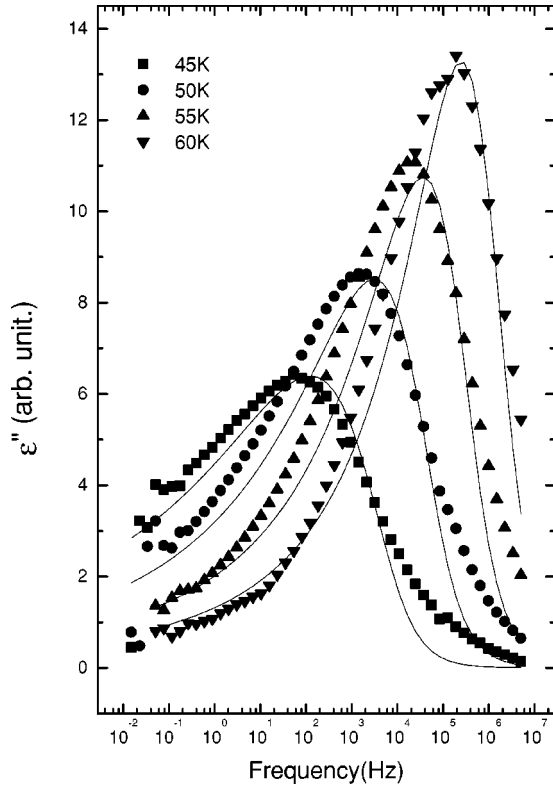


FIG. 6. Comparison of the experimental dielectric permittivity of the DRADP dipole glass with the numerically obtained permittivity function (based on the correlated domain model) at four different temperatures.

lated domain decreases with decreasing temperature and explains the general tendency of the variation in experimentally obtained Debye frequencies.

The temperature dependence of the dynamic dipolar correlation is also presented in Fig. 7(b) by plotting the coefficient C as a function of temperature. It has a plateau value of around 20 at near 60 K and then increases monotonously as temperature decreases. The estimated positive values of C with the absence of a ‘‘crossover’’ correspond to the existence of a long tail at the low-frequency side of $\epsilon''(\omega)$ spectrum and suggest an existence of the Curie-von Schweider (CvS) type power law relaxation. These results are in sharp contrast to the negative values of C and, thus, to the existence of a long tail in the high-frequency side of $\epsilon''(\omega)$ observed in a series of glass-forming materials.^{15,31,32}

According to the study done by Chamberlin,¹⁵ the estimated values of C for Salol, a glass-forming liquid, are negative and vary from -1.5 to -4.7 as temperature decreases from 290 to 219 K. Similar relaxation behavior was also observed in other glass-forming liquids that include propylene glycol (PRGL) and N -methyl- ϵ -caprolactam (NMEC).³² These observations suggest that the dynamic dipolar correlation of the DRADP is significantly stronger than that of glass-forming liquids but the freezing temperature of the DRADP dipole glass (below 40 K; Fig. 7) is significantly lower than those of glass-forming materials.³² In case of $\text{KTaO}_3:\text{Li}$, a kind of quadrupole glass, Chamberlin¹⁸ reported that the Dixon-Nagel scaling³¹ did work pretty well. In this system, values of the correlation coefficient C are

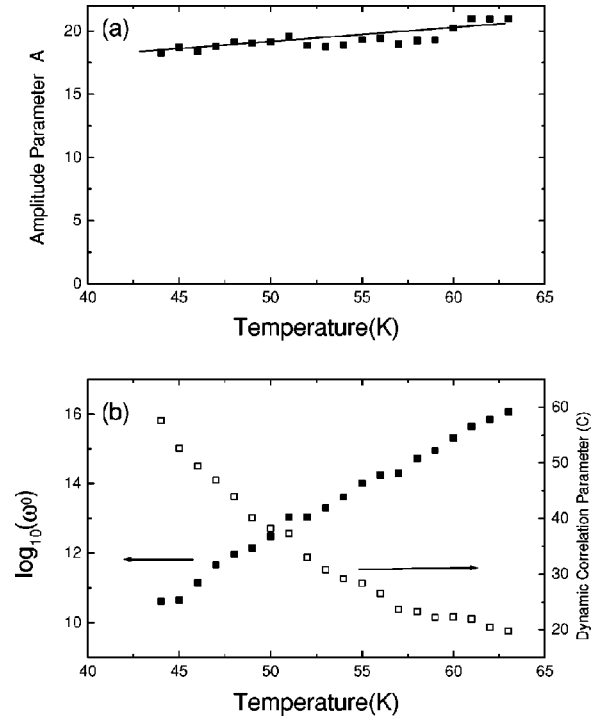


FIG. 7. Analysis of dielectric relaxation parameters used in the correlated domain model: (a) the amplitude parameter A as a function of temperature, (b) the temperature dependence of the Debye frequency and the degree of the dynamic dipolar correlation (C).

greater than zero but they are still much smaller than those for the DRADP estimated here.

As shown in Fig. 6, the scaling does not work satisfactorily for the DRADP. This is mainly caused by the fact that the broadness of the dielectric permittivity spectrum is significantly greater than those of other glass-like dipolar systems. In the Chamberlin’s model, the broadness of the dielectric permittivity is directly related to the asymmetry of $\epsilon''(\omega)$ spectrum, and the broadness cannot be established without imposing this asymmetry. Therefore, more satisfactory numerical fittings obtained in Salol and $\text{KTaO}_3:\text{Li}$ quadrupole glass can be attributed to the smaller broadness in $\epsilon''(\omega)$ spectrum.

However, there are a couple of ways toward the improvement. One is the introduction of a temperature-dependent parameter that can give an arbitrary broadness in a Poisson-type distribution. Then, the size distribution function of the dynamically correlated domain would depend on temperature. The other is the change in the form of kernel other than the Debye kernel. This strategy is based on the fact that the Cole-Davidson kernel is broader than the simple Debye kernel.

V. CONCLUSIONS

The low-frequency dielectric relaxation of the DRADP dipole glass was investigated by examining the complex dielectric permittivity and the relaxation-time distribution function $g(\tau)$ above the glass freezing temperature. We have shown that none of the well-known Debye-type relaxation functions that include the Cole-Cole, Cole-Davidson, and KWW functions does adequately describe the observed di-

electric relaxation behavior of the DRADP. We have then applied and examined the Chamberlin's correlated domain model as a possible description of the DRADP dipole glass. Although there are some discrepancies between the experimental data and the computational results based on the correlated domain model, both of them have the same general tendencies : (i) a long tail at the lower-frequency side and (ii) increase in the asymmetry of $\epsilon''(\omega)$ spectrum with decreasing temperature. The observed discrepancies were then explained in terms of the broadness or, equivalently, the asym-

metry of the dielectric response function of the DRADP dipole glass.

ACKNOWLEDGMENTS

This work was supported by the Korea Science and Engineering Foundation (RCDAMP-1998). Support from the Basic Science Research Institute (BSRI) at POSTECH is also appreciated.

-
- ¹E. Courtens, J. Phys. (France) Lett. **43**, L199 (1982).
²E. Courtens, Phys. Rev. Lett. **52**, 69 (1984).
³R. Blinc, D. C. Ailion, B. Günther, and S. Žumer, Phys. Rev. Lett. **57**, 2826 (1986).
⁴V. H. Schmidt, S. Waplak, S. Hutton, and P. Schnackenberg, Phys. Rev. B **30**, 2795 (1984).
⁵S. Iida and H. Terauchi, J. Phys. Soc. Jpn. **52**, 4044 (1983).
⁶E. Matsushita and T. Matsubara, J. Phys. Soc. Jpn. **55**, 666 (1986).
⁷R. Pirc, B. Tadic, and R. Blinc, Phys. Rev. B **36**, 8607 (1987).
⁸R. Blinc, J. Dolinšek, R. Pirc, B. Tadić, B. Zalar, R. Kind, and O. Liechti, Phys. Rev. Lett. **63**, 2248 (1989).
⁹P. He, J. Phys. Soc. Jpn. **60**, 313 (1991).
¹⁰F. L. Howell, N. J. Pinto, and V. H. Schmidt, Phys. Rev. B **46**, 13 762 (1992).
¹¹Z. Kutnjak, C. Filipić, A. Levstik, and R. Pirc, Phys. Rev. Lett. **70**, 4015 (1993).
¹²Z. Kutnjak, R. Pirc, A. Levstik, I. Levstik, C. Filipić, R. Blinc, and R. Kind, Phys. Rev. B **50**, 12 421 (1994).
¹³Bog-Gi Kim and Jong-Jean Kim, Phys. Rev. B **55**, 5558 (1997).
¹⁴R. V. Chamberlin and D. N. Haines, Phys. Rev. Lett. **65**, 2197 (1990).
¹⁵R. V. Chamberlin, Phys. Rev. Lett. **66**, 959 (1991).
¹⁶R. V. Chamberlin, Phys. Rev. B **48**, 15 638 (1993).
¹⁷R. V. Chamberlin, R. Böhmer, E. Sanchez, and C. A. Angell, Phys. Rev. B **46**, 5787 (1992).
¹⁸R. V. Chamberlin, Europhys. Lett. **33**, 545 (1996).
¹⁹P. Debye, *Polar Molecules* (Dover, New York, 1945).
²⁰K. S. Cole and R. H. Cole, J. Chem. Phys. **9**, 341 (1941).
²¹C. P. Lindsey and G. D. Patterson, J. Chem. Phys. **73**, 3348 (1980).
²²C. J. Dias, Phys. Rev. B **53**, 14 212 (1996).
²³F. Kohlrausch, Pogg. Ann. Phys. und Chem. **119**, 352 (1863); see also F. Kohlrausch, Prakt. Phys. (Stuttgart) **I**, 129 (1955).
²⁴G. Williams and D. C. Watts, Trans. Faraday Soc. **66**, 80 (1970).
²⁵D. W. Davidson and R. H. Cole, J. Chem. Phys. **19**, 1417 (1951).
²⁶S. Havriliak and S. Negami, Polymer **8**, 161 (1967).
²⁷K. Liedermann and A. Loidl, J. Non-Cryst. Solids **155**, 26 (1993).
²⁸F. Alvarezm, A. Alegria, and J. Colmenero, Phys. Rev. B **44**, 7306 (1991).
²⁹F. Alvarezm, A. Alegria, and J. Colmenero, Phys. Rev. B **47**, 125 (1993).
³⁰W. H. Press, S. A. Teukolsky, W. T. Vetterling, and B. P. Flannery, *Numerical Recipes in C* (Cambridge University Press, Cambridge, 1992).
³¹P. K. Dixon, L. Wu, S. R. Nagel, B. D. Williams, and J. P. Carini, Phys. Rev. Lett. **66**, 960 (1991).
³²C. Hansen, R. Richert, and E. W. Fisher, J. Non-Cryst. Solids **215**, 293 (1997).